SYNCHROTRON TOPOGRAPHIC AND DIFFRACTOMETRIC STUDIES OF BURIED LAYERED STRUCTURES OBTAINED BY IMPLANTATION WITH SWIFT HEAVY IONS IN SILICON SINGLE CRYSTALS

W. Wierzchowski[a #], K. Wieteska[b], D. Żymierska[c], W. Graeff[d], T. Czosnyka[e], and J. Choiński[e]

[a]*Institute of Electronic Materials Technology, ul. Wólczyńska 133, PL 01-919 Warsaw, Poland*
[b]*Institute of Atomic Energy, PL-05-400 Świerk, Poland*
[c]*Institute of Physics of PAS, Al. Lotników 32/46, PL-02-668 Warsaw, Poland*
[d]*HASYLAB at DESY, Notkestr. 85, D-22603 Hamburg, Germany*
[e]*Heavy Ion Laboratory, University of Warsaw, ul. Pasteura 5a, PL-02-093 Warsaw, Poland*

Abstract: A distribution of crystallographic defects and deformation in silicon crystals subjected to deep implantation (20-50 μm) with ions of the energy of a few MeV/amu is studied. Three different buried layered structures (single layer, binary buried structure and triple buried structure) were obtained by implantation of silicon single crystals with 184 MeV argon ions, 29.7 MeV boron ions, and 140 MeV argon ions, each implantation at a fluency of 1×10^{14} ions cm-^{2}. The implanted samples were examined by means of white beam X-ray section and projection topography, monochromatic beam topography and by recording local rocking curves with the beam restricted to 50×50 μm^2. The experiment pointed to a very low level of implantation-induced strain (below 10^{-5}). The white beam Bragg case section experiment revealed a layer producing district black contrast located at a depth of the expected mean ion range. The presence of these buried layered structures in studied silicon crystals strongly affected the fringe pattern caused by curvature of the samples. In case of white beam projection and monochromatic beam topographs the implanted areas were revealed as darker regions with a very tiny grain like structure. One may interpret these results as the effect of considerable heating causing annihilation of point defects and formation of dislocation loops connected with point defect clusters.

Topograficzne i dyfraktometryczne synchrotronowe badania struktur z warstwami zagrzebanymi otrzymanymi przez implantację prędkimi jonami ciężkimi w monokryształach krzemu
Streszczenie: Badano rozkład defektów krystalograficznych i deformacji w krzemie poddanym głębokiej implantacji (20 - 50 μm) jonami o energii kilku MeV/amu. Trzy struktury odpowiednio z pojedynczą, podwójną i potrójną warstwą zagrzebaną otrzymano przez implantację kryształów krzemu jonami argonu o energii 184 MeV, boru o energii 29,7 MeV i argonu o energii 140 MeV do fluencji 1×10^{14}cm^{-2} dla każdego pierwiastka. Próbki badano za pomocą przekrojowej i projekcyjnej topografii synchrotronowej w wiązce białej, topografii w wiązce monochromatycznej oraz rejestracji lokalnych krzywych odbicia w wiązce 50×50 μm^2. Badania wykazały bardzo niski poziom odkształceń wywołanych implantacją (poniżej 10^{-5}). Topografia przekrojowa ujawniła warstwę wywołującą wyraźny czarny kontrast na topogramie położoną na głębokości oczekiwanego zasięgu jonów. Obecność warstw zagrzebanych silnie wpływała na układ prążków interferencyjnych wywoływanych przez krzywiznę próbek. W przypadku topografii projekcyjnej w wiązce białej i topografii w wiązce monochromatycznej obszar implantowany był ujawniany jako obszar ciemniejszy z delikatnym kontrastem ziarnistym. Wyniki te można interpretować jako efekt silnego wzrostu temperatury powodującego anihilację par defektów punktowych i formowanie się pętli dyslokacyjnych związanych ze skupiskami defektów punktowych.

[#] Corresponding author: Tel.: +48 22 835-3041, fax: +48 22 834-9003., E-mail: wierzc_w@itme.edu.pl

1. Introduction

The investigation of silicon implanted with swift heavy ions of several MeV/amu energy has both cognitive and practical aspects. Swift heavy ions impinging on a single crystal far from the direction of channelling stripe electrons from the atoms lying on their tracks. Ionised atoms repel each other creating the structural disturbance along the track of incident particle. The type and concentration of defects vary with depth due to the different dominating interaction processes of ions with the solid. Swift heavy ion beams cause less damage within the near-surface shot-through region, but they can create buried layers in a target, (see *e.g.* Ref. [1]). Observation of latent tracks in silicon single crystals is very difficult [2-6]. However, X-ray techniques succeeded to detect significant deformation of the crystal lattice induced by ion implantation [7-9].

High energy significantly increases the penetration range of ions and number of generated defects enabling the observation of many physical phenomena. That in particular concerns the studies of implanted layers by means of X-ray diffraction methods, which are more effective in this case. Some high-energy ion implantations are used in the technology of semiconductor devices, but also the explanation of related physical phenomena may be useful for more efficient controlling of various implantation processes used in technology.

The aim of the research is to study the distribution of crystallographic defects and deformation in silicon crystals subjected to deep implantation (20-50 mm) with ions of the energy of a few MeV/amu. The X-ray investigations of silicon implanted with such high energy Ar and Kr ions were previously described in [10-12]. It is also well known that the thermal annealing strongly affects the state of point defects introduced by the implantation causing partial annihilation of vacancies and interstitials [13, 14].

The present investigation includes a number of complementary X-ray methods exploring both white and monochromatic synchrotron radiation.

2. Experimental

Dislocation-free silicon single crystals were grown by the Czochralski method. Four (001) oriented thin plates were cut from it. Three samples were implanted at a K=160 cyclotron at Heavy Ion Laboratory of the University of Warsaw [15], the sample 1 was kept as a reference. The beam current was equal to 50 enA. The implantation was performed at room temperature by uniformly defocused beam.

In order to perform the implantation, we have designed and constructed a special irradiation chamber, which permits one to irradiate a selected domain on the surface of a studied crystal without necessity of opening the chamber. Such construction makes possible to repeat the implantation process many times without renewal pumping. The chamber is shown in Fig. 1. The chamber was used for implantation of (001) oriented silicon samples with three ion beams, each at a fluency of 1×10^{14} ions·cm^{-2}. First, samples 2, 3, and 4 were irradiated with 4.6 MeV/amu (total energy equal to 184 MeV) Ar ions, then samples 3 and 4 were bombarded by 2.7 MeV/amu (total energy equal to 29.7 MeV) B ions, and lastly only the sample 4 was implanted with 3.5 MeV/amu (total energy equal to 140 MeV) Ar ions. The mean ion ranges, calculated by means of the TRIM programme [16, 17], are equal to 48.0 μm, 44.3 μm, and 35.3 μm, respectively. This way we obtained three different buried layered structures in silicon single crystal plates: i) single buried layer, ii) binary buried structure, and iii) triple buried structure (see Table 1).

The implanted samples were examined at HASYLAB using both monochromatic and white synchrotron beam. The monochromatic beam investigations were performed at E2 station using the 0.1115 nm radiation monochromatised by the successive symmetrical 333 and 511 symmetrical reflection from piezoelectrically stabilized silicon crystals. The experiments included taking i) local rocking curves with the beam restricted to 50×50 μm^2 and ii) monochromatic beam topographs at chosen point of the 004 rocking curve.

The white beam investigations were performed at F1 experimental station in back reflection geometry with a relatively small glancing angle of 5^o. Both projection and section topographs were taken. A single exposed white beam pattern consisted of certain number of Laue spots, each of them being a topograph in reflection from different crystallographic planes. In case of section topographs, a beam front was formed by a fine 5 μm slit. The section topographs were taken both at short (10 cm) and relatively large (30 cm) film-to-crystals distances to separate the effects coming from different depth location and from strain-induced lattice deformation.

Fig. 1. Special irradiation chamber, enabling to irradiate different places on the surface of a studied crystal without necessity of opening.

Table 1. Studied silicon samples with buried layered structures.

Sample	First Ar ion implantation (184 MeV): buried layer at a depth of [μm]	B ion implantation (29.7 MeV): buried layer at a depth of [μm]	Second Ar ion implantation (140 MeV): buried layer at a depth of [μm]	Result
Sample 1	-	-	-	As grown
Sample 2	48.0	-	-	Single buried layer
Sample 3	48.0	44.3	-	Binary buried structure
Sample 4	48.0	44.3	35.3	Triple buried structure

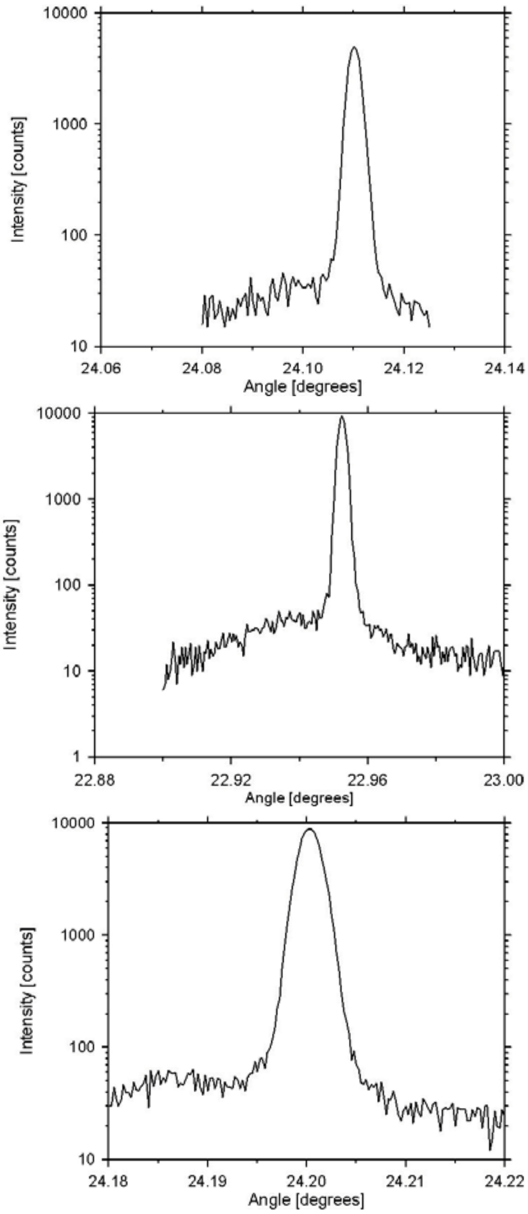

Fig. 2. The experimental synchrotron rocking curves in 004 symmetrical reflections of double and triple implanted silicon exhibiting only a small increase of FWHM of the main peak:

- single implantation with 4.6 MeV/amu (total energy equal to 184 MeV) Ar ions (upper),
- double implantation with 4.6 MeV/amu (total energy equal to 184 MeV) Ar ions and 2.7 MeV/amu (total energy equal to 29.7 MeV) B ions (middle),
- triple implantation with 4.6 MeV/amu (total energy equal to 184 MeV) Ar ions, 2.7 MeV/amu (total energy equal to 29.7 MeV) B ions, and 3.5 MeV/amu (total energy equal to 140 MeV) Ar ions (lower).

3. Results and discussion

The rocking curves shown in Fig. 2 exhibit only slight broadening of the main peak, and no other maxima are observed. Together with that in Fig. 3 we observe an additional contrast coming from the implanted region with a very faint grain-like structure. That points a very low level of implantation-induced strain (less than 10^{-5}). The enhanced contrast in the implanted region seems to be caused by used not exactly parallel setting of multi-crystal arrangement. It may be also noticed that the peak broadening seems to be highest in case of triple implanted sample (Fig. 2, lower curve).

The interesting feature of the Bragg-case white beam section topographs are interference fringes, shown in Fig. 4, analogous to those described in [18, 19] and theoretically explained by Chukhowski and Petrashen [20]. In the present case, the crystal bending caused by imperfect etching of the rear surface after grinding is the reason of formation of the fringes. It may be noticed that the fringe pattern from the implanted region is significantly changed (similarly as it was observed in [21]), but the amount of interference effects is much lower in the present case. One may in particular observe a distinct black stripe probably caused by the mostly damaged layers. In most cases we observe a single line, and the contribution from different ions is poorly resolved.

Similarly as in case of monochromatic beam topographs, the white beam topograph reveals black contrast in the implanted region with a faint grain-like structure. That is representatively shown in Fig. 5 in case of sample triple implanted with 4.6 MeV/amu Ar ions, 2.7 MeV/amu B ions, and 3.5 MeV/amu Ar ions.

The above-presented results are attributed to significant heating during the implantation process causing the healing of the introduced point defects, which usually cause a significant strain in as-implanted samples [21]. It was calculated with TRIM programme that for such high-energy ions used in the present case the amount of created point defects is at least 30 times greater than the amount of ions. It is also probable that the black stripe observed in Bragg-case section topographs and faint grain-like structure in white beam section and monochromatic beam topographs are caused by small dislocation loops created in the annealing process.

4. Conclusions

The aim of the present paper was the study of different buried layered structures (single layer, binary buried structure, and triple buried structure) obtained by implantation of silicon single crystals with three kinds of swift ion, namely of 184 MeV Ar ions, 29.7 MeV B ions, and 140 MeV Ar ions, each at a fluency of 1×10^{14} ions·cm^{-2}.

The monochromatic beam experiment pointed to a very low level of implantation induced strain (less than 10^{-5}), producing only a certain broadening of the rocking curve maximum, and enhanced black contrast of the implanted regions.

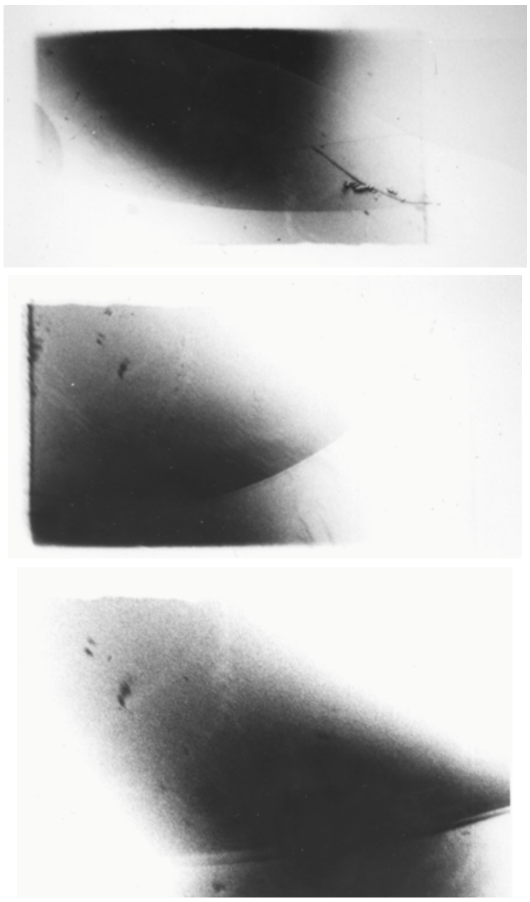

Fig. 3. Monochromatic beam topographs [a] of the silicon samples with buried layered structures: single buried layer (upper), double buried layer (middle), triple buried structure (lower).

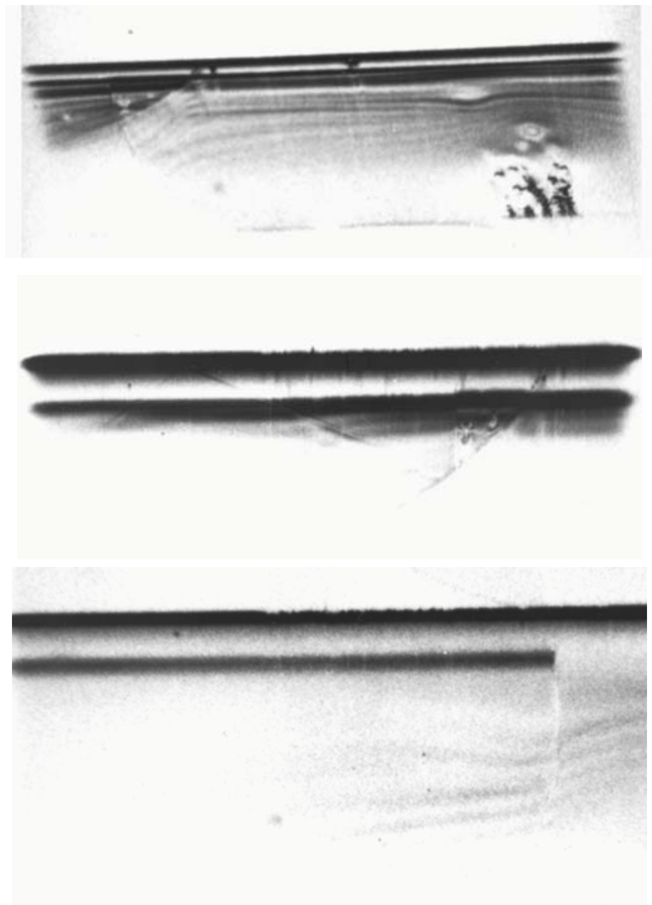

Fig. 4. Bragg-case section topographs [a] of the high energy Ar and B ion implantation to silicon (energies of ion beams the same as in fig. 2): sample 2 (upper), sample 3 (middle), sample 4 (lower).

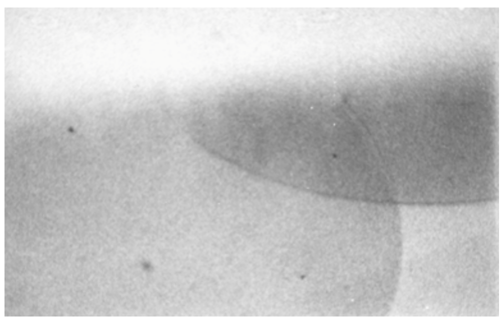

Fig. 5. Bragg case projection topograph[a] of silicon sample 4.

[a] The width of all topographs is equivalent to ~7 mm.

The white-beam Bragg case section experiment revealed a layer producing a distinct black contrast located at the expected mean ion range. The presence of this layer strongly affected the fringe pattern caused by bending of the sample.

The white beam projection and monochromatic beam topographs the implanted areas were revealed as darker regions with a very tiny grain like structure.

One can interpret these results as the effect of significant heating of the samples during implantation, causing annihilation of point defects and formation of dislocation loops connected with point defect clusters.

References

[1] W. Wesh, O. Herre, P.I. Gaiduk, E. Wendler, S. Klaumünzer, P. Meier, *Nucl. Instrum. Meth. Phys. Res. B* **146** (1998) 341.

[2] M. Levalois, P. Bogdanski, M. Toulemonde, *Nucl. Instrum. Meth. Phys. Res. B* **63** (1992) 14.

[3] E. Balanzat, *Radiat. Effects. Defects Solids* **126** (1993) 97.

[4] S. Furuno, H. Otsu, K. Izui, *Nucl. Instrum. Meth. Phys. Res. B* **107** (1996) 223.

[5] P. Sigmund, *Nucl. Instrum. Meth. Phys. Res. B* **135** (1998) 1.

[6] A. Dunlop, G. Jaskierowicz, S. Della-Negra, *Nucl. Instrum. Meth. Phys. Res. B* **146** (1998) 302.

[7] J. Auleytner, J. Bąk-Misiuk, Z. Furmanik, J. Morawiec, *Cryst. Res. Technol.* **23** (1988) K20.

[8] J. Auleytner, V.I. Khrupa, L.I. Datsenko, S.M. Krasulya, M.J. Skorookhod, *Acta Phys. Polon. A* **89** (1996) 301.

[9] D. Żymierska, J. Auleytner, K. Godwod, J. Domagała, L. Datsenko, J. Choiński, *J. Alloys Comp*. **328** (2001) 237.

[10] A. Barbu, J.C. Jousset, G. Martin, M. Toulemonde, *Nouvelles des GANIL* **9** (1985) 16.

[11] J.N. Górecka, J. Auleytner, *phys. stat. sol. (a)* **137** (1993) 309.

[12] J. Auleytner, *Nucl. Instrum. Meth. Phys. Res. B* **87** (1994) 124.

[13] D. Żymierska, K. Godwod, J. Adamczewska, J. Auleytner, J. Choiński, K. Regiński, *Acta Phys. Polon. A* **101** (2002) 743.

[14] W. Wierzchowski, K. Wieteska, J. Auleytner, W. Graeff, D. Żymierska, *J. Alloys Compds* **382** (2004) 146.

[15] *Annual Reports of the Heavy Ion Laboratory* (University of Warsaw, Warsaw 1993-2005).

[16] J.P. Biersack, L.G. Haggmark, *Nucl. Instrum. Meth. Phys. Res.* **174** (1980) 257.

[17] J.F. Ziegler, J.P. Biersack, U. Littmark: in: "*The Stopping and Range of Ions in Solids,* J.F. Ziegler (Ed.), (Pergamon Press, New York 1985).

[18] P. Zaumseil, *Krist. Technik* **13** (1978) 983.

[19] J. Bak-Misiuk, J. Gronkowski, J. Härtwig, W. Wierzchowski, *phys. stat. sol. (a)* **99** (1987) 345.

[20] F.N. Chukhovski, P.V. Petrašen, *Acta Crystallogr. A* **44** (1988) 8.

[21] K. Wieteska, W. Wierzchowski, W. Graeff, *Il Nuovo Cimento* **19 D** (1997) 239.